

Experimental ratchet effect in superconducting films with periodic arrays of asymmetric potentials

J. E. Villegas,¹ E. M. Gonzalez,¹ M. P. Gonzalez,¹ J. V. Anguita,² and J. L. Vicent¹

¹*Departamento Fisica Materiales, Facultad CC. Fisicas, Universidad Complutense, 28040 Madrid, Spain*

²*Instituto Microelectronica de Madrid, Centro Nacional Microelectronica, CSIC, Isaac Newton 8, P.T.M. Tres Cantos, 28760 Madrid, Spain*

(Received 4 June 2004; revised manuscript received 8 September 2004; published 26 January 2005)

A vortex lattice ratchet effect has been investigated in Nb films grown on arrays of nanometric Ni triangles, which induce periodic asymmetric pinning potentials. The vortex lattice motion yields a net dc voltage when an ac driving current is applied to the sample and the vortex lattice moves through the field of asymmetric potentials. This ratchet effect is studied taking into account the array geometry, the temperature, the number of vortices per unit cell of the array, and the applied ac currents.

DOI: 10.1103/PhysRevB.71.024519

PACS number(s): 74.78.-w, 05.60.-k, 74.40.+k

Feynman used, in his Lectures on Physics,¹ a ratchet to show how anisotropy never could lead to net motion in an equilibrium system. Since then, asymmetric sawtooth potentials are called ratchet potentials and, in general, a device with broken inversion symmetry is called a ratchet device. The ratchet effect occurs when asymmetric potentials induce outward particle flow under external fluctuations in the lack of any driving direct outward forces. The ratchet effect changes an ac source in a dc one. Ratchet effect spans from Nature phenomena to laboratory fabricated devices. In a ratchet, the energy necessary for net motion is provided by raising and lowering the barriers and wells, either via an external time-dependent modulation, for example an ac current injected in a superconducting film with asymmetric pinning centers,² or by energy input from a nonequilibrium source, such as a chemical reaction, as for instance in biological motors.³ During the past years, ratchet effect has called the attention of many researchers. A state of the art on the related topics Brownian motion and ratchet potential could be found in Ref. 4.

The use of ratchetlike pinning potentials in superconductors has been the subject of theoretical approaches which deal with very different topics, for instance, to remove flux trapped in superconducting devices,⁵ fluxon optic,⁶ logic devices,⁷ etc. From the experimental point of view, some progress has been reported related to superconducting circuits,⁸⁻¹⁰ and very recently vortex motion ratchet effect has been reported in superconducting films with artificially fabricated arrays of asymmetric pinning centers.² In the present paper, we will address some of the properties of this superconducting ratchet effect. We will explore the dependence of the ratchet with the applied alternating current, the array shape, the temperature, and the number of vortices per array unit cell. We will show that periodic asymmetric potentials are crucial to produce the ratchet behavior, that the effect is enhanced decreasing the temperature, and finally, that the effect decreases when the applied magnetic field (number of vortices per unit cell of the array) increases.

The paper is organized as follows: First, we will summarize some results on the behavior of vortex lattice on arti-

cially induced pinning potentials. After this, we will present the fabrication method and main characteristics of the films. Finally, the experimental ratchet effect results will be showed and discussed.

The dynamics of vortex lattice on artificially induced symmetric pinning potentials has received a lot of attention during past years. Different shapes of pinning centers and arrays, and different materials have been explored from the experimental as well as the theoretical points of view. As it has been shown,¹¹ the dc magnetoresistance of superconducting thin films with periodic arrays of pinning centers show minima when the vortex lattice matches the unit cell of the array. These minima are sharp (strong reduction of the dissipation) and equal spaced (two neighbor minima are always separated by the same magnetic field value). In the case of square arrays of nanostructured pinning centers, minima appear at applied magnetic fields $H_m = n(\Phi_0/a^2)$, where a is the lattice parameter of the square array and $\Phi_0 = 2.07 \times 10^{-15}$ Wb is the magnetic flux quantum. Hence, the number of vortices n per array unit cell can be known by simple inspection of the dc magnetoresistance $R(H)$ curves, in which the first minimum corresponds to one vortex per unit cell, the second minimum to two vortices per unit cell, and so on. Moreover, the ratio between the dimension of the pinning center and the superconducting coherence length governs the maximum number of vortices that could be pinned in each one of the magnetic centers.¹² Therefore, we know, for selected values of the applied magnetic field, how many vortices are per unit cell and where they are, this is, if they are interstitial vortices or vortices in the pinning centers. Other interesting effects induced by these periodic potentials on the vortex lattice behavior are changes in the vortex lattice symmetry,¹³ channeling effects in the vortex motion,¹⁴ and effects related to the interplay between these artificial periodic pinning centers and the intrinsic random pinning centers of the sample.¹⁵ Concerning the pinning mechanisms and the magnetic state of the pinning centers, it has been reported¹⁶ that, in our samples (Nb thin films with arrays of very thin Ni magnetic pinning centers), the pinning mechanisms are the result of the interplay among different magnetic mechanisms. The magnetic state of the Ni pinning centers has been

checked by magnetic-force microscopy experiments,¹⁷ which show that the magnetization in the Ni triangles is in-plane aligned. For the magnetotransport experiments reported here, the applied magnetic field is always perpendicular to the film plane, and its value is much smaller than the magnetic field needed to change the in-plane magnetization,¹⁷ which therefore remains invariable during our experiments. Some experimental work related to the dependence of pinning mechanisms on the magnetization of the pinning centers has been reported for instance by Morgan and Ketterson¹⁸ and Van Bael *et al.*¹⁹ In the former case the pinning centers, thick Ni dots, completely perforated the Nb film and had perpendicular magnetization. The latter authors change the magnetic state of the Co dots applying a magnetic field parallel to the superconducting Pb film plane. Finally, another point that is worthwhile to notice is the number of vortices that could be pinned in the pinning centers, and whether they exist as multiple-quantized vortices or in single vortex states. Regarding the first topic, Hoffmann *et al.*¹² have experimentally studied the number of vortices per array unit cell and per pinning site, taking into account the dots size and the unit cell parameters in Nb film with Ni arrays of different dot sizes. Concerning the single vortex states vs. multiple-quantized flux lines, in the case of superconducting thin films with arrays of holes (*antidots*), it is generally assumed that multiquanta vortices appear.²⁰ Theoretical calculations for mesoscopic superconducting flat samples with triangular shapes, for example, have also showed that in some cases multiquanta vortex configurations are energetically favorable.²¹ However, so far we know, there are not calculations that matches our situation, i.e., a triangular magnetic pinning trap covered by a superconducting thin film.

Electron beam lithography, magnetron sputtering and ion etching techniques are used to fabricate Nb thin films (100 nm thickness) grown on arrays of Ni triangles of thickness 40 nm. Si(100) is used as substrate. A cross-shape patterned bridge of 40 μm wide allows us injecting current into the sample. More fabrication and characterization details have been reported elsewhere.²

Figure 1 shows the dc voltage drop V_{dc} measured along the x axis due to the ac current density $J=J_{ac}\sin(\omega t)$ ($\omega=10$ kHz) injected along the x axis in two samples A, Fig. 1(a), and B, Fig. 1(b), with different arrays and with one vortex per unit cell. Although the samples are quite different the experimental results are similar. In summary, the ac current density yields an ac Lorentz force on the vortices that is given by $\vec{F}_L=\vec{J}\times\vec{n}\phi_0$ (where \vec{n} is a unitary vector parallel to the applied magnetic field), but the time averaged driving force on vortices is $\langle F_L \rangle=0$. From the expression for the electric field $\vec{E}=\vec{B}\times\vec{v}$ (with \vec{B} the applied magnetic field and \vec{v} the vortex-lattice velocity), we get that the dc voltage drop V_{dc} measured along the direction of the injected current is proportional to the average vortex-lattice velocity $\langle v \rangle$ in the direction of the ac driving force; in particular $V_{dc}=\langle v \rangle dB$ (where d is the distance between contacts and B the applied magnetic induction). For an ac current input (or ac driving force), the output is a nonzero dc voltage V_{dc} . This means that a net vortex lattice flow ($\langle v \rangle \neq 0$) arises from the ac

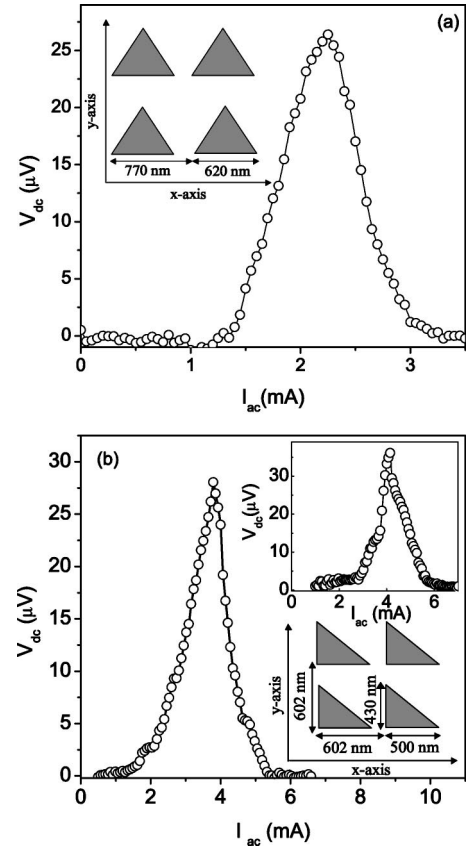


FIG. 1. (a) V_{dc} output versus ac input amplitude I_{ac} for sample A, with current injected along x axis, at $T=0.989T_c$ and applied magnetic field $H=32$ Oe ($n=1$). *Inset*: Sketch of the array of triangles and their sizes for sample A. (b) V_{dc} output versus ac input amplitude I_{ac} for sample B, with current injected along x axis at $T=0.984T_c$ and applied magnetic field $H=54$ Oe ($n=1$). *Upper inset*: V_{dc} output versus ac input amplitude I_{ac} for sample B, with current injected along the y axis, at $T=0.984T_c$ and applied field $H=54$ Oe ($n=1$). *Lower inset*: Sketch of the array of triangles and their sizes for sample B.

driving force ($\langle F_L \rangle=0$), what shows that the array of Ni triangles induces a ratchet potential landscape for the vortex lattice. The magnitude of V_{dc} output depends on the amplitude of the ac current input J_{ac} : V_{dc} peaks as a function of the ac input amplitude. This behavior agrees with results obtained from numerical simulations of vortex dynamics in asymmetric potentials.²² As the ac amplitude increases, the net velocity increases monotonically from zero up to the maximum value. From this point the effect progressively smears out as stopping forces become negligible in comparison with the ac drive amplitude.

The inset of Fig. 1(b) shows the same experiment for sample B, but now the dc voltage drop V_{dc} is measured along the y axis. This voltage is due to the ac current density $J=J_{ac}\sin(\omega t)$ injected along the y axis. In sample A the dc signal is zero along the y axis,² while in sample B the dc voltage shows similar values than in the perpendicular direction [Fig. 1(b)]. The ratchet effect along y axis vanishes in the A sample because the vortex lattice is flowing on an array of symmetric periodic potentials. However, in sample B the

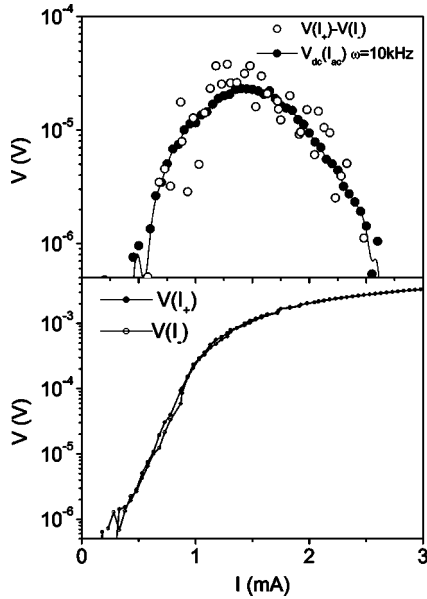


FIG. 2. (Upper panel) ac ratchet effect $V_{dc}(I_{ac})$ for sample A (black dots), and dc ratchet effect obtained by subtracting $V(I_+) - |V(I_-)|$ (white dots), at applied magnetic field $H=64$ Oe, and $T=0.995T_c$. (Lower panel) $V(I_+)$ and $|V(I_{dc-})|$ at $H=64$ Oe and $T=0.995 T_c$.

pinning potential is also asymmetric along the x axis, thus yielding a ratchet effect along this direction. Although for sample B the pinning potential is asymmetric along the x and y directions, these directions are not exactly equivalent, since the intertriangles distances and triangle sidelengths are not equal along both directions [see sketch on Fig. 1(b)]. As has been recently shown²³ the interpinning traps distance is a very critical parameter for vortex-lattice dynamics, and the shape and size of the asymmetric pinning traps are also crucial to the ratchet effect and they can strongly modify the vortex trajectories, as has been shown in numerical simulations.²² Therefore, the different shapes and slightly different values observed in the $V_{dc}(I_{ac})$ curves along the x and y directions in sample B were expected provided the different pinning landscape existing along the x and y axis. A more detailed explanation of the particular differences and features observed in the $V_{dc}(I_{ac})$ curves would require a numeric simulation specific to this pinning potential geometry.

To underline that the asymmetric potential is the main ingredient of the ratchet effect, we have tested the ratchet system in the *adiabatic* limit ($\omega \rightarrow 0$) by injecting dc current. Figure 2 shows the comparison between the ac ratchet effect, at the highest frequency that is attainable in our experimental set up ($\omega = 10$ kHz), and the pure dc (*adiabatic*) experiment. Here the *ratchet signal* is extracted from dc $I(V)$ curves: after a dc current is applied, first in the $+x$ -axis $V(I_+)$, and then in the $-x$ axis $V(I_-)$, both curves are subtracted and the net voltage is $V = V(I_+) - |V(I_-)|$. We can see from Fig. 2 that the dc experiment mimics the ac data, that is, the curve shape, amplitude, and current window where the ratchet effect occurs with ac drive. Moreover, from Fig. 2(b) one can clearly see that the ratchet effect is observed for ac (or dc) current amplitudes above the dc critical current. A frequency

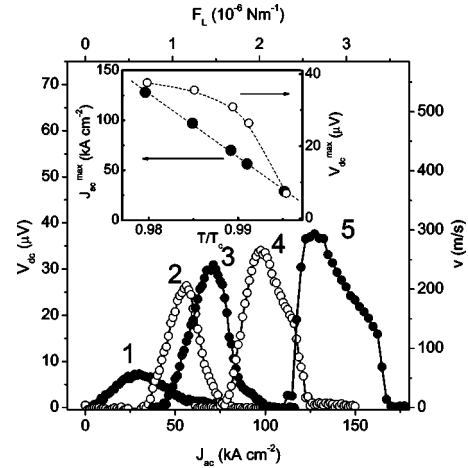


FIG. 3. V_{dc} output versus J_{ac} amplitude input (or equivalent net velocity v versus ac force amplitude F_L) for sample A, with J injected along the x axis, at applied magnetic field $H=32$ Oe ($n=1$) and temperatures (1) $T=8.300$ K, (2) $T=8.265$ K, (3) $T=8.250$ K, (4) $T=8.214$, and (5) $T=8.170$ K. Sample $T_c=8.340$ K. *Inset*: Maximum dc rectification V_{dc}^{max} and ac current input at which this is achieved J_{ac}^{max} as a function of the reduced temperature T/T_c , for sample A, with J injected along x axis, at applied magnetic field $H=32$ Oe ($n=1$).

dependence of the ratchet effect would be only expected at much higher frequencies. At high enough frequencies vortices could travel distances comparable to the separation a between triangles in the period of the ac drive. As it was found in numeric simulations, in such regime commensurate lock-in transitions should develop, giving raise to plateaus in the $V_{dc}(I_{ac})$ curves and a nonmonotonic dependence $V_{dc}(\omega)$.²² At very high ac frequency, the travel of vortices could be even shorter than intertriangles separation, and in such case no dc signal would develop. All those features are not observed in our experimental data since, even considering the net velocity of the vortex lattice, always in the range 10–100 m/s (see Figs. 3 and 4), and the highest attainable frequency in our experiments (10 kHz), the travel distance of vortices in a period is about $l \sim v/\omega \geq 10^3 \mu\text{m}$, much larger than any of the array characteristic lengths ($\leq 1 \mu\text{m}$). Nevertheless, the general trends of our experimental data can be compared to the trends observed in the numerical simulations in Ref. 22. In this work, it is said that the *adiabatic* $V_{dc}(I_{dc})$ curves embed all $V_{dc}(I_{ac})$ curves simulated for higher frequencies, as earlier demonstrated.²⁴ That is, even though some features observed only for $V_{dc}(I_{ac})$ curves simulated at high frequencies are not seen for the calculation in the *adiabatic* limit, as for instance the plateaus due to the lock-in transitions cited above, the overall $V_{dc}(I_{ac})$ curve at any frequency is contained within the area delimited below the *adiabatic* $V_{dc}(I_{dc})$. A clear image of this can be viewed in Fig. 7(b) of Ref. 22. Therefore, for instance, even if the frequency range of our experimental data is much lower than the one used in those numerical simulations, a qualitative comparison between the temperature dependence observed in simulations and our experimental data could be done.

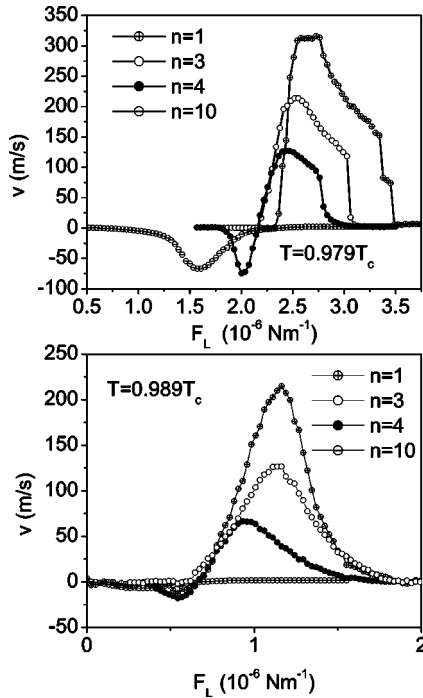


FIG. 4. (*Upper panel*) For sample A, net velocity of the vortex lattice v as a function of the ac Lorentz force amplitude F_L , for a frequency $\omega=10$ kHz, $T=0.979T_c$ and different numbers of vortices per unit cell n . (*Lower panel*) For sample A, net velocity of the vortex lattice v as a function of the ac Lorentz force amplitude F_L , for a frequency $\omega=10$ kHz, $T=0.989T_c$ and different numbers of vortices per unit cell n .

Figure 3 shows the temperature dependence of the ratchet effect, in sample A, with the ac current injected parallel to the triangle basis (x axis) and one vortex per pinning site. The temperature has several effects on the ratchet behavior: on one hand, the effect is enhanced, since the maximum rectification value V_{dc}^{max} monotonically increases as temperature is decreased, and the shape of the peak gets steep. These trends are illustrated in the inset of Fig. 3. In this inset, the maximum in the rectification V_{dc}^{max} is depicted as a function of the reduced temperature. As can be seen, V_{dc}^{max} grows fast with decreasing temperature, and afterwards increases more slowly and finally seems to saturate. This behavior could be related to the *thermal noise*,²² which assists vortex motion through fluctuations, and that washes out potential asymmetry at temperatures very close to T_c , strongly reducing the magnitude of the ratchet effect. Thermal noise disappears as temperature is lowered from T_c , which produces the fast increase in the rectification, while further temperature reduction has a less pronounced effect. On the other hand, the ac current amplitude at which the maximum in dc rectification voltage develops, J_{ac}^{max} , is shifted towards lower values as temperature decreases. This is also shown in the inset of Fig. 3. The origin of the shifting of the $V_{dc}(J_{ac})$ curves is related to the enhancement of pinning potential with decreasing temperature, which yields higher stopping forces on the vortex lattice. The value of the critical current increases as temperature decreases: values for $H=32$ Oe are around 25 kA cm^{-2} (1 mA in our bridge) at $T=0.99 T_c$ and 100 kA cm^{-2} (4 mA)

at $T=0.98 T_c$. These are typical values of critical current in this kind of patterned Nb films.^{12,16,25} It is remarkable that the effect of temperature on our experimental ratchet is very similar to the one produced by disorder in the array of asymmetric pinning centers on the simulated ratchet effect calculated by Zhu *et al.*²² Curves simulated for higher array disorder (Fig. 11 of Ref. 22) mimics our experimental curves for higher temperatures, in the sense that both simulated and experimental curves get much smoother than the steep curves experimentally observed at low temperatures (similar to simulated curves for low disorder in the array). According to this fact, the enhancement of the ratchet effect due to the decrease of temperature is similar to the one observed in simulations for higher array order. On the other hand, the ratchet effect vanishes when the temperature, or the array disorder, increases. These features in common should be explored deeper.

Finally, the effects of increasing the applied magnetic field and its temperature dependence have been studied. From the filling factor and experimental measurements² the maximum number of vortices pin in one triangle is three. The question of whether or not multiquanta vortices develop is not clear; the experimental ratchet effect reported here cannot shed much light into this question since, qualitatively, a similar behavior could be expected assuming one multiquanta vortex or multiple single vortices, at least if we consider that multiple single vortices pinned in the same triangle move at the same time. This seems a reasonable scenario given the similar behavior of $v(F_L)$ curves for $n=1$, $n=2$, or $n=3$ (see Figs. 2 and 4). The main difference between them is that increasing the number of vortices the magnitude of $v(F_L)$ is reduced, because the stronger vortex-vortex interactions compete with the pinning potential, smoothing its asymmetry. A numerical calculation of vortex trajectories to be compared with experimental results could be helpful in order to tackle the question of the single or multiquanta vortex states.

Increasing even more the applied magnetic yields interstitial vortices (vortices not pinned in Ni triangles), what produces a striking effect.² The polarity of the ratchet signal changes when going from three vortices per unit cell (everyone of the vortices in the triangles) to four vortices per unit cell (the first interstitial vortex appears). The reversed polarity of the ratchet is explained because the interstitial vortices feel a ratchet potential reverse and weaker than the pinned vortices, since the asymmetry is induced for those by vortex-lattice interactions. Then a negative signal appears at low drives since the interstitial vortices move first, because they need smaller applied force than the pinned vortices to yield a dc voltage.

Figure 4 shows this behavior for two different temperatures. Again we can notice that decreasing the temperature the ratchet effect is enhanced for both types of vortices, although the distortion on the signal shape only appears in the case of pinned vortices, since they are the vortices in the ratchet traps, and the interstitial vortices feel the weaker ratchet effect through the vortex lattice interaction.

In closing, applying an alternating current to a Nb film growth on Ni arrays with asymmetric pinning potentials

yields net vortex motion, whose sense is governed by the asymmetry of the pattern. The most outstanding experimental facts of this superconducting experimental ratchet are as follows.

(i) The origin of the ratchet effect is the asymmetry of the potentials that assemble the array.

(ii) The ratchet effect is monotonically smoothed increasing the temperature.

(iii) At constant temperature and driving force, the ratchet effect reverses and decreases amplitude increasing

the applied magnetic field. That is, the number of vortices per unit cell of the array and amplitude of the dc ratchet voltage.

(iv) At constant temperature and applied magnetic field, the ratchet effect vanishes increasing the driving force on the vortex lattice.

We want to thank Spanish CICYT MAT2002-04543 and R. Areces Foundation. E.M.G. wants to thank Ministerio de Educación y Ciencia for a Ramon y Cajal contract.

-
- ¹R. P. Feynman, R. B. Leighton, and M. Sands, *The Feynman Lectures on Physics* (Addison-Wesley, Reading, MA, 1963), Chap. 46.
- ²J. E. Villegas, S. Savel'ev, F. Nori, E. M. Gonzalez, J. V. Anguita, R. Garcia, and J. L. Vicent, *Science* **302**, 1188 (2003).
- ³A. Yildiz, M. Tomishige, R. D. Vale, and Paul R. Selvin, *Science* **303**, 676 (2004).
- ⁴Special issue on Ratchets and Brownian Motors: Basic, Experiments and Applications, edited by H. Linke, *Appl. Phys. A: Mater. Sci. Process.* **75**, 167 (2002).
- ⁵C. S. Lee, B. Janko, L. Derényi, and A. L. Barábasi, *Nature (London)* **400**, 337 (1999).
- ⁶J. F. Wambaugh, C. Reichhardt, C. J. Olson, F. Marchesoni, and F. Nori, *Phys. Rev. Lett.* **83**, 5106 (1999).
- ⁷M. B. Hastings, C. J. Olson Reichhardt, and C. Reichhardt, *Phys. Rev. Lett.* **90**, 247004 (2003).
- ⁸S. Weiss, D. Koelle, J. Müller, R. Gross, and K. Barthal, *Europhys. Lett.* **51**, 499 (2000).
- ⁹G. Carapella and G. Costabile, *Phys. Rev. Lett.* **87**, 077002 (2001).
- ¹⁰E. Trías, J. J. Mazo, F. Falo, and T. P. Orlando, *Phys. Rev. E* **61**, 2257 (2000).
- ¹¹J. I. Martín, M. Velez, J. Nogués, and Ivan K. Schuller, *Phys. Rev. Lett.* **79**, 1929 (1997).
- ¹²A. Hoffmann, P. Prieto, and Ivan K. Schuller *Phys. Rev. B* **61**, 6958 (2000).
- ¹³J. I. Martin, M. Velez, A. Hoffmann, I. K. Schuller, and J. L. Vicent, *Phys. Rev. Lett.* **83**, 1022 (1999).
- ¹⁴M. Velez, J. I. Martín, M. I. Montero, I. K. Schuller, and J. L. Vicent, *Phys. Rev. B* **65**, 104511 (2002).
- ¹⁵M. Velez, D. Jaque, J. I. Martin, F. Guinea, and J. L. Vicent, *Phys. Rev. B* **65**, 094509 (2002).
- ¹⁶J. I. Martin, M. Velez, A. Hoffmann, I. K. Schuller, and J. L. Vicent, *Phys. Rev. B* **62**, 9110 (2000).
- ¹⁷A. Asenjo *et al.* (unpublished).
- ¹⁸D. J. Morgan and J. B. Ketterson, *Phys. Rev. Lett.* **80**, 3614 (1998).
- ¹⁹M. J. Van Bael, K. Temst, V. V. Moshchalkov, and Y. Bruynseraede, *Phys. Rev. B* **59**, 14 674 (1999).
- ²⁰A. I. Buzdin, *Phys. Rev. B* **47**, 11 416 (1993); V. V. Moshchalkov, M. Baert, V. V. Metlushko, E. Roseel, M. J. Van Bael, K. Temst, and R. Jonckheere, *ibid.* **54**, 7385 (1996).
- ²¹B. J. Baelus and F. M. Peeters, *Phys. Rev. B* **65**, 104515 (2002).
- ²²B. Y. Zhu, F. Marchesoni, V. V. Moshchalkov, and F. Nori, *Phys. Rev. B* **68**, 014514 (2003).
- ²³J. E. Villegas, E. M. Gonzalez, M. I. Montero, Ivan K. Schuller, and J. L. Vicent, *Phys. Rev. B* **68**, 224504 (2003).
- ²⁴L. R. Bartussek, P. Hänggi, and J. G. Kissner, *Europhys. Lett.* **28**, 459 (1994).
- ²⁵D. Jaque, E. M. González, J. I. Martín, J. V. Anguita, and J. L. Vicent, *Appl. Phys. Lett.* **81**, 2851 (2002).